ACTA ONCOLOGICA, 2016
VOL. 55, NO. 5, 647–651
http://dx.doi.org/10.3109/0284186X.2015.1105383

Taylor & Francis
Taylor & Francis Group

LETTER TO THE EDITOR

Evaluation of different CT lung anatomies for proton therapy with pencil beam scanning delivery, using a validated non-rigid image registration method

Elisa Scalco[a], Marco Schwarz[b], Marina Sutto[c], Daniele Ravanelli[b], Francesco Fellin[b], Giovanni M. Cattaneo[d] and Giovanna Rizzo[a]

[a]Istituto di Bioimmagini e Fisiologia Molecolare (IBFM), CNR, Segrate (MI), Italy; [b]Centro di Protonterapia, Azienda Provinciale per i Servizi Sanitari (APSS), Trento, Italy; [c]Università degli studi di Trento, Trento, Italy; [d]Dipartimento di fisica medica, Ospedale San Raffaele, Milano, Italy

To the Editor,

Proton therapy (PT) is in principle an interesting option for the treatment of lung cancer patients [1]; in fact, PT offers the theoretical possibility to design and deliver better dose distributions than with photons, thus allowing a possible improvement of the clinical results [2]. However, the dose distributions achievable with protons are very sensitive to changes in radiological depths along the beam path [3]. In particular, the treatment of moving target in highly heterogeneous tissue, as it occurs in lung radiotherapy (RT), is a great challenge, and large errors leading to underdose of the tumor or overdose of healthy tissues are possible [4].

The optimization of dose planning based on four-dimensional computed tomography (4DCT) acquisition techniques combined with deformable image registration methods can help in the choice of the best performing lung anatomy for the treatment planning optimization. By this procedure, the comparison between CT anatomies can thus be performed quantitatively through dose accumulation, estimating the effective dose delivered on target volume and critical organs [5]. In the last years, some works have already studied the impact of different treatment plan anatomies on the effective dose delivered during the breathing cycle in a proton treatment delivered with broad beams [4,5]. To our knowledge, the suitability of these methods for PT with scanning beams has not been tested yet. The additional degrees of freedom available with pencil beam scanning (PBS) with respect to broad beam techniques are such that a more conformal dose can be designed. This, in turn, makes PBS dose distributions more sensitive with respect to several aspects of the treatment chain, including the anatomy representation used for planning.

The aim of this study was thus to evaluate different CT lung anatomies for dose planning in PT delivered with PBS.

Materials and methods

Image dataset

Six patients with advanced stage lung cancers, lymphnodal and/or mediastinal involvement and peak-to-peak gross tumor volume (GTV) motion amplitude of approximately 10 mm were selected for this study (more details are reported in Table I in Supplementary Material, available online at http://www.informahealthcare.com).

All these patients underwent 4D positron emission tomography (PET)-CT scan with a PET-CT scanner (Discovery STE/690, GE Healthcare). Each 3D lung acquisition corresponded to a respiratory phase; the entire breathing cycle was divided in six phases. Contours of GTV and lungs were manually delineated by an experienced radiation oncologist in all breathing phases.

Treatment planning

Two-field plans were designed using the Xio TPS (Elekta, release 4.80) with simultaneous multifield optimization [also known as intensity modulated PT (IMPT)] [6]; more details are reported in Supplementary Material) on different anatomy representations defined as follows:

(1) average intensity projection CT (Avg-IP CT): the value of each voxel is calculated as the average over the breathing phases;
(2) maximum intensity projection CT (MIP CT): the value of each voxel is calculated as the maximum over the breathing phases;
(3) mid-exhale CT (MidEx CT): is the mid-exhale phase, selected as the one where tumor position was in its cranial-caudal (CC) time-averaged position during the respiratory cycle;
(4) average CT with internal target volume (ITV) filled with MIP density (Avg-ITVMIP CT): the value of each voxel is calculated as the average over the breathing phases, except for the voxels within the ITV, whose values have been replaced by a higher-density value, which is the maximum over the breathing phases;
(5) mid-exhale CT with ITV filled with MIP density (MidEx-ITVMIP CT): MidEx represents the mid-exhale phase and ITV voxels have been replaced with the corresponding MIP voxels.

CONTACT Correspondence: M. Schwarz marco.schwarz@apss.tn.it Centro di Protonterapia, Azienda Provinciale per i Servizi Sanitari (APSS), via al Desert 14, Trento, Italy
Supplemental data for this article can be accessed http://dx.doi.org/10.3109/0284186X.2015.1105383

Table I. Target dose coverage, homogeneity index and conformity index for the different planning strategies evaluated on the first two patients.

3DCT anatomy	Patient no.	$V_{95\%}$ [%]	$V_{107\%}$ [%]	$D_{1\%}$ [Gy(RBE)]	$D_{99\%}$ [Gy(RBE)]	HI [%]	CI
Avg-IP CT	1	96.3	0.0	70.9	65.3	5.3	1.9
	2	85.2	0.0	71.3	57.9	13.0	1.8
MidEx CT	1	48.6	0.0	70.7	55.3	18.6	1.1
	2	89.8	0.0	71.5	64.1	8.3	1.7
MidEx-ITVMIP CT	1	70.4	0.0	72.0	57.9	14.0	1.5
	2	99.7	31.0	77.4	69.6	8.3	2.9
MIP	1	100.0	0.0	73.3	68.9	3.9	2.6
	2	97.4	32.0	83.1	63.3	18.8	3.4
	3	96.7	78.3	91.3	62.8	29.3	3.8
	4	99.9	89.9	85.0	70.7	11.9	3.2
	5	99.8	57.4	80.9	69.3	13.0	4.0
	6	100.0	69.6	80.1	72.3	8.1	3.3
	Average	*99.0*	*54.5*	*82.3*	*67.9*	*14.2*	*3.4*
Avg-ITVMIP	1	88.4	0.0	70.9	63.5	7.7	1.8
	2	99.7	16.8	76.9	68.5	7.7	2.6
	3	99.9	17.5	77.4	68.4	9.2	3.0
	4	97.2	0.0	71.7	64.2	5.5	1.7
	5	99.7	2.4	75.2	67.6	7.9	2.5
	6	98.6	0.0	73.3	65.8	6.4	2.4
	Average	*97.3*	*6.1*	*74.2*	*66.3*	*7.4*	*2.3*

In a first phase all five anatomies were tested and compared on two patient datasets, then the two best performing anatomies were used for the remaining four patients.

The target was chosen to be the ITV [7] for all the planning anatomies, with no additional margins, as the focus of this work was to address only the breathing component of the geometrical uncertainties and not setup or range errors. In clinical practice, of course, the margins set in this study would be combined with additional margins for setup errors and interfraction organ motion (e.g. changes in the respiratory baseline).

Dose accumulation over respiratory cycle and dose evaluation

The optimized dose distributions obtained from the treatment plans designed on the basis of different artificial anatomies were recalculated on all six frames of the 4DCT. Each dose distribution was deformed on the reference phase by applying the deformation field estimated by image registration, using the free form deformation (FFD) method based on cubic B-splines, and minimizing mutual information (MI) as cost function. Details about the algorithm implementation can be found in a previous work of our group [8], while the evaluation of the image registration accuracy is widely described in the Supplementary Material. Finally, the deformed doses were accumulated over the respiratory cycle to yield the accumulated 4D-dose.

To investigate the effect of the different planning anatomies on the effective delivered dose over the respiratory cycle, the accumulated 4D-doses were evaluated in terms of GTV coverage and organs at risk (OARs) sparing. In particular, homogeneity index (HI) and conformity index (CI) were calculated as:

$$HI = \frac{D_{5\%} - D_{95\%}}{D_{prescription}} \quad (4)$$

where $D_{5\%}$ and $D_{95\%}$ is the dose delivered to the 'hottest' and 'coldest' 5% of the GTV volume, respectively; and

$$CI = \frac{V_{body95\%}}{V_{target}} \quad (5)$$

where $V_{body95\%}$ is the volume of tissue encompassed by the 95% isodose level and V_{target} is the GTV.

Results

Results of the dose planning on the five 3D CT lung anatomies evaluated on two subjects are summarized in Table I (Patients 1 and 2) and shown as representative dose-volume histograms (DVHs) in Figure 1; it has been found that proton plans based on Avg-IP CT and MidEx CT are not robust against respiratory motion as GTV coverage is not achieved in the cumulative dose distribution. Avg-ITVMIP and MidEx-ITVMIP methods ensured target coverage with good sparing of healthy lung tissue only for one patient, whose respiratory amplitude was approximately 1 cm. The other patient, whose target motion amplitude exceeded 1.5 cm, showed unacceptably poor GTV dose coverage. The MIP method guaranteed dose coverage to the GTV but was very conservative for one patient.

Based on these results, MIP and Avg-ITVMIP were the two planning strategies candidates to be tested on the remaining four patients (Figure 2 shows an example for the first two patients).

Results on the next four patients are also reported in Table I (Patients 3–6), confirming what was found in the previous two subjects. In particular, dose distributions planned with MIP strategy were highly inhomogeneous within the target, however, all the indices to the lungs were below the prescribed limits, even if hotspots were present in the ipsilateral lung.

Considering Avg-ITVMIP, cumulative dose distributions were very homogeneous in the target ($HI = 7.4 \pm 1.3\%$), so that cumulative dose maps resembled the nominal ones more than cumulative dose distributions from MIP plans did. Hot spots in the target were present in a significant percentage only in one patient ($V_{107\%}$=17.5% in Patient 3), which were anyway well below the corresponding values in MIP plan. Very good conformity was achieved ($CI = 2.3 \pm 0.5$) and all indices to the lung parenchyma were below the prescribed limits.

Discussion

In this work we evaluated five different CT lung anatomies for treatment planning in PT with PBS. For this evaluation, a dose accumulation procedure over the entire breathing cycle was

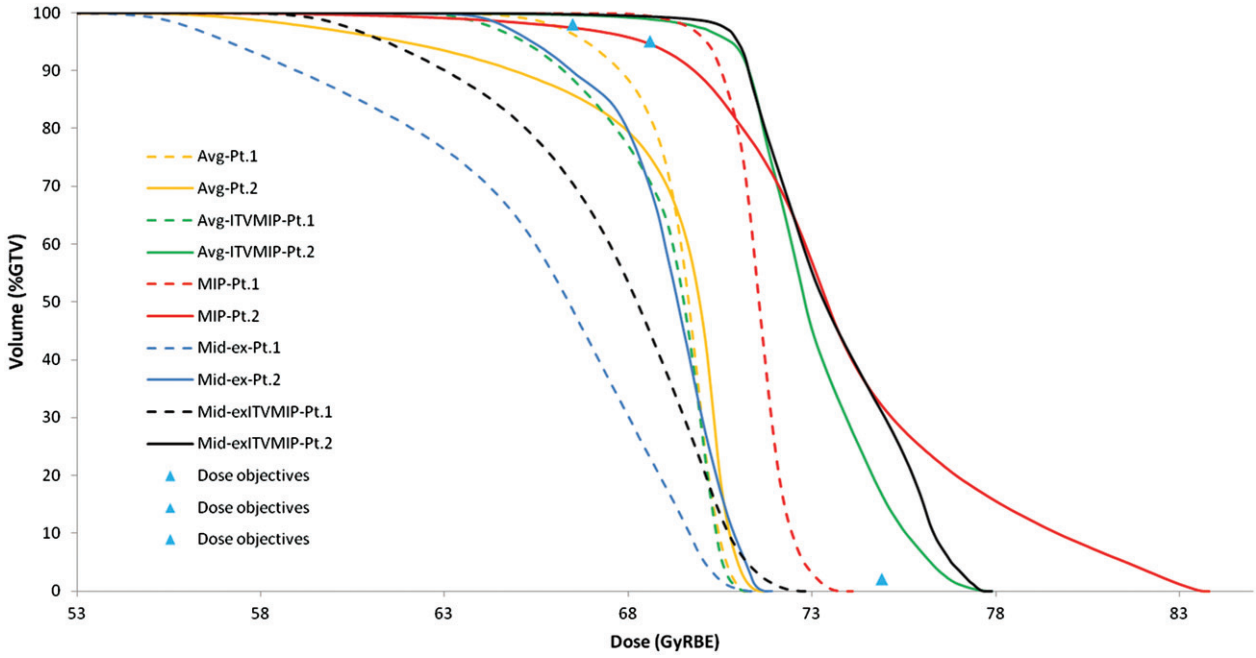

Figure 1. Cumulative dose-volume histograms of GTV for the first two patients, estimated from all the five proposed anatomies (Avg, Avg-ITVMIP, MIP, MidEx, MidEx-ITVMIP). The prescribed dose is also shown.

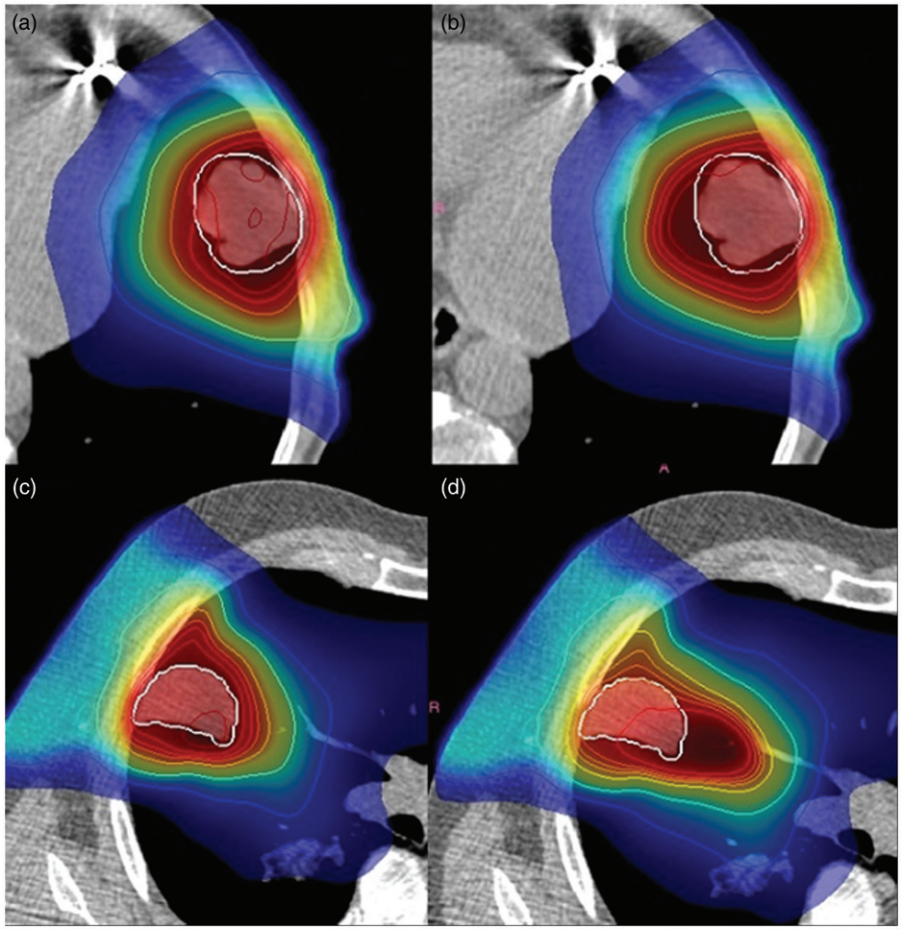

Figure 2. Cumulative dose distributions on two cases, using the two best performing anatomies. a) Avg-ITVMIP, study 1; b) MIP, study 1; c) Avg-ITVMIP, study 2; d) MIP, study 2. Isodose lines [% of 70 Gy(RBE), from the outside in]: 20%, 50%, 80%, 90%, 95%, 100%, 107%.

employed, starting from a 4DCT image set, and based on a validated deformable image registration method.

In this study, the best anatomy representation for planning was Avg-ITVMIP. In fact, while both Avg-ITVMIP and MIP ensure good target coverage, the latter was associated to significant overdosages in the target volume and a lack of dose conformity.

In our patient anatomies, the only OAR distally and laterally to the target was the lung, so the effect of overdosage to the OARs did not significantly deteriorate the dose indices for such organ, whose risk of complication is essentially associated to the mean dose. However, if OARs with a small volume effect such as spinal cord and esophagus were close to the target, the overdosages associated to the MIP plan may have been clinically unacceptable.

Our results are in line with what has been suggested in past studies [5,9], even though MIP appeared to provide superior results in a more recent publication [4].

We should consider that the aforementioned studies were based on PT delivered with scattered beams, where the dose distribution is shaped via field-specific hardware (apertures and compensators). As a consequence, such dose distributions typically lack the dose conformity achievable with PBS. In addition, we focused on the effect of the respiratory motion only and we therefore planned the dose distributions on the ITV, rather than on a volume with additional margins with respect to it [e.g. the planning target volume (PTV)]. By planning on the PTV and simulating the breathing motion only, as it has been done in some studies (e.g. [10]), one may take advantage of the margins meant for setup errors (i.e. the ITV to PTV margins) and use them instead to compensate for the effect of breathing motion.

The additional degrees of freedom of PBS, where position, energy and number of protons can be set individually for every pencil beam, allows for dose distributions that are more conformal (sometimes significantly so). Such dose distributions therefore pose more demands on the accuracy of the anatomy representation, as the dose is tightly shaped around the designed target and one cannot use the lack of conformity as a sort of additional safety margin. In literature there are examples of approaches where the range uncertainty in beam scanning charged particle therapy is tackled in the optimization process (e.g. [11]), while in our study we focused on the stage of anatomy representation, and relied on standard commercially available tools for the optimization.

It is worth noticing that, by design, our approach does not rely on margins. This choice is due to two main reasons:

(1) Our aim was to study only the impact of intrafraction respiratory motion on dose distributions, while margins are typically adopted to correct for setup errors.
(2) Even more importantly, margins are in general not the most appropriate tools to compensate for geometrical uncertainties in PT, where margin-less planning approaches, such as robust optimization (see e.g. [12]), are preferable. One can therefore think about a combination between our approach and robust optimization, where the former compensates for intrafraction motion, while the latter deals with range and setup uncertainties.

In this study we did not address the issue of 'interplay effects', i.e. of dosimetric effects due to the interference between breathing motion and beam delivery. Although in theory one may include interplay effects in planning, currently the most feasible approach is probably to take care of interplay at the delivery stage, i.e. with techniques such as rescanning, either layer-by-layer or volumetric [13]. In addition, it is possible [14] that, even in case of treatments in free breathing, the interplay effects may be negligible for the lesions analyzed in this study, which are treated with conventional fractionation and are not at the same time small and subject to large respiratory motion.

In conclusion, MIP and Avg-ITVMIP were found to assure good target coverage and normal tissue spare; however MIP has led to overdosage to the GTV and low conformity. The MIP method guaranteed dose coverage to the GTV but was very conservative for one patient: the accumulated dose showed hot spots (>110% prescription dose) in both the GTV and the ipsilateral lung, and a large volume of unspecified normal tissues to receive medium to high doses.

At least in theory, neither MIP nor Avg-ITVMIP is the ideal solution for all possible combinations of tumor sizes and locations and amplitude of the breathing motion. For instance, using the MIP to outline an ITV is problematic if the tumor is adjacent to the diaphragm and the Avg-ITVMIP CT strategy may not be able to ensure target coverage in small tumors.

For our patient dataset, Avg-ITVMIP was the best CT planning anatomy able to correct intrafraction motion, when PBS is used for PT.

References

1. Widesott L, Amichetti M, Schwarz M. Proton therapy in lung cancer: Clinical outcomes and technical issues. A systematic review. Radiother Oncol 2008;86:154–64.
2. Zhang X, Li Y, Pan X, Xiaoqiang L, Mohan R, Komaki R, et al. Intensity-modulated proton therapy reduces the dose to normal tissue compared with intensity-modulated radiation therapy or passive scattering proton therapy and enables individualized radical radiotherapy for extensive stage IIIB non-small-cell lung cancer: A virtual clinical study. Int J Radiat Oncol Biol Phys 2010;77:357–66.
3. Engelsman M, Schwarz M, Dong L. Physics controversies in proton therapy. Semin Radiat Oncol 2013;23:88–96.
4. Zhao L, Sandison GA, Farr JB, Hsi WC, Li XA. Dosimetric impact of intrafraction motion for compensator-based proton therapy of lung cancer. Phys Med Biol 2008;53:3343.
5. Kang Y, Zhang X, Chang JY, Wang H, Wei X, Liao Z, et al. 4D Proton treatment planning strategy for mobile lung tumors. Int J Radiat Oncol Biol Phys 2007;67:906–14.
6. Lomax A. Intensity modulation methods for proton radiotherapy. Phys Med Biol 1999;44:185.
7. Morgan-Fletcher S. Prescribing, recording and reporting photon beam therapy (Supplement to ICRU Report 50), ICRU Report 62. ICRU, pp. ix 52, 1999 (ICRU Bethesda, MD). Br J Radiol 2001;74:294.
8. Faggiano E, Cattaneo GM, Ciavarro C, Dell'Oca I, Persano D, Calandrino R, et al. Validation of an elastic registration technique to estimate anatomical lung modification in non-small-cell lung cancer tomotherapy. Radiat Oncol 2011;6:31–40.
9. Engelsman M, Rietzel E, Kooy HM. Four-dimensional proton treatment planning for lung tumors. Int J Radiat Oncol Biol Phys 2006;64:1589–95.
10. Li H, Liu W, Park P, Matney J, Liao Z, Chang J, et al. Evaluation of the systematic error in using 3D dose calculation in scanning beam proton therapy for lung cancer. J Appl Clin Med Phys 2014;15:4810.

11. Graeff C, Durante M, Bert C. Motion mitigation in intensity modulated particle therapy by internal target volumes covering range changes. Med Phys 2012;39:6004–13.
12. Fredriksson A, Forsgren A, Hårdemark B. Minimax optimization for handling range and setup uncertainties in proton therapy. Med Phys 2011;38:1672–84.
13. Bernatowicz K, Lomax A, Knopf A. Comparative study of layered and volumetric rescanning for different scanning speeds of proton beam in liver patients. Phys Med Biol 2013;58:7905.
14. Li Y, Kardar L, Li X, Li H, Cao W, Chang JY, et al. On the interplay effects with proton scanning beams in stage III lung cancer. Med Phys 2014;41:021721.